Springer

KSME

Journal of Mechanical Science and Technology 31 (5) (2017) 2443~2449
www.springerlink.com/content/1738-494x(Print)/1976-3824(Online)
DOI 10.1007/s12206-017-0442-4

Ag-water nanofluid flow over an inclined porous plate embedded in a non-Darcy porous medium due to solar radiation †

Tanmoy Chakraborty[1,*], Kalidas Das[2] and Prabir Kumar Kundu[3]

[1]*Department of Mathematics, Techno India College of Technology, Newtown, Kolkata 700156, W.B., India*
[2]*Department of Mathematics, A.B.N.Seal College, Cooch Behar, W.B., India*
[3]*Department of Mathematics, Jadavpur University, Kolkata 700032, W.B., India*

(Manuscript Received May 14, 2016; Revised September 28, 2016; Accepted January 17, 2017)

Abstract

The heat absorber uses in solar power plants have generally low energy adaptation owing to large emissive losses at high temperature. Recently, nanofluid based solar energy absorber have acknowledged immense scientific curiosity to competent share and store the thermal energy. Here we examine theoretically the natural convective flow of an Ag nanoparticle based nanofluid flow along an inclined flat sheet embedded in a Darcy-Forchheimer permeable medium coexistence of solar radiation. By use of similarity transformations, the fundamental partial differential system and boundary conditions are tackled numerically using Runge-Kutta Gill based shooting procedure. The impacts of governing parameters upon the flow, temperature, Nusselt number and skin friction coefficient are represented tabular as well as in graphical form.

Keywords: Ag-water nanofluid; Darcy-Forchheimer porous medium; Solar radiation; Suction/injection

1. Introduction

The most essential resource of energy of this planet is the solar energy. Solar energy never consumes and owing to lack of the fuel will arise in near future; we will be strained to change our powering ways to maintain the daily necessities and amenities. On the dependency of the resource of light and heat from the sun, a variety of technologies namely solar heating, solar electricity, solar photo voltaic cells etc have been raised. Thus, the applications of solar based technologies magnetize much more consideration in many branches of applied physics. Hunt [1] first introduced the concept of employing the particles to absorb solar energy. A suspensions of nano sized solid metallic particles in liquid identified as nanofluid, have received extensive attention for their characteristics. Many research workers [2-4] have established the effectiveness of higher heat transport rate owing to the high thermal conductivity of nanofluids. The influences of solar radiation on the flow as well as on heat transport with different flow situations are found in the open literature [5-7].

Heat transport owing to natural convection is quite significant for its extensive usage in industry and engineering system. Plentiful research works have been worked out by several researchers on natural convection flow in nanofluids considering different flow condition in different geometries. Some contributions on this topic are noticed in the recent studies [8-11]. An evaluation work on free convective heat transport in nanofluids was studied by Karak and Pramuanjaroenkij [12]. Natural convective flow of a naofluid with several flow situation along horizontally placed surface are discussed in the recent works [13-15].

The transport of heat owing to convection and fluid flow embedded in a permeable medium is a phenomenon of great scientific interest because of its extensive usage in science as well as in engineering and geophysical fields. The former researches on heat transfer of natural convective flow over permeable medium were found in the investigations of Cheng and Minkowycz [16], Lai and Kulacki [17]. Most of the former investigations over permeable medium have applied the Darcy's law which depicts that the volume averaged velocity is correlated to the pressure gradient. When the permeable medium is surrounded by an resistant wall, elevated flow rates or the medium possess non-uniform porosity diameter distribution, the Darcy law is not fitting. Thus, it is essential to introduce an additional term with Darcian term to analyze the flow behavior properly on porous medium [18, 19]. Kaviany [20] also used the Darcy Brinkman model is to evaluate the impacts of boundary and inertia forces over an impermeable flat plate. At high flow situation, the effect of inertia is neces-

*Corresponding author. Tel.: +91 8902470845
E-mail address: tanmoyc88@gmail.com
† Recommended by Associate Editor Jaeseon Lee

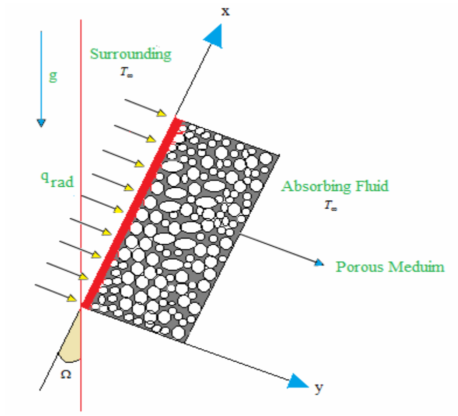

Fig. 1. Flow configuration and coordinate system.

sary to be considered and that can be arranged by imposing an additional velocity-squared term in the momentum equation, identified as Forchheimer extension [21]. The model of Darcy-Forchheimer in the heat and mass transport problem in a fluid-saturated permeable medium was incorporated by many of researchers [22-25].

The purpose of this present article is to extend the work of Mukhopadhyay et al. [24] by considering Ag-water nanofluid flow over an inclined porous flat plate embedded in a Non-Darcy permeable medium owing to solar radiation.

2. Mathematical formulation

We presume a steady, free convection two dimensional flow of an incompressible viscous Ag-water nanofluid along an inclined, solar-radiation heated flat plate embedded in a fluid soaked porous medium (Fig. 1). The temperature near the surface takes the constant value T_w while the ambient value is T_∞. Owing to the heating on the inclined plate by solar radiation, nanofluid takes up the heat and transferred it to the surrounds. The solid absorbent medium takes up the radiant heat flux of strength q_{rad} and transmits it to the stream by convection. The leading differential equation of the fluid motion depends on Darcy-Forchheimer model, which accounts for the pull exerted by the permeable surface and the effect of inertia. Under these postulations, the primary equations can be explained as:

$$\frac{\partial u}{\partial x}+\frac{\partial v}{\partial y}=0 \tag{1}$$

$$u\frac{\partial u}{\partial x}+v\frac{\partial u}{\partial y}= \frac{1}{\rho_{nf}}\left[\mu_{nf}\frac{\partial^2 u}{\partial y^2}+(\rho\beta)_{nf}\,g(T-T_\infty)\cos\Omega\right] -\frac{v_f}{k}(u-u_\infty)-\frac{k'}{\sqrt{k}}(u^2-u_\infty^2) \tag{2}$$

$$u\frac{\partial T}{\partial x}+v\frac{\partial T}{\partial y}=\alpha_{nf}\frac{\partial^2 T}{\partial y^2}-\frac{1}{(\rho C_p)_{nf}}\frac{\partial q_{rad}}{\partial y}. \tag{3}$$

Here u, v stands for the component of velocity in the x, y direction respectively, $v_f=\mu_f/\rho_f$ symbolizes the kinematic viscosity. $k=k_0x$ exemplifies the Darcy permeability of the absorbent medium with the initial permeability k_0; $k'=\frac{k_0'}{\sqrt{x}}$ denotes the Forchheimer resistance factor with Forchheimer constant k_0'; u_∞ specifies the free stream speed and C_p signifies the specific heat at constant pressure. By the use of Rosseland estimation for radiation we can express $q_{rad}=-\frac{4\sigma}{3k^*}\frac{\partial T^4}{\partial y}$ where σ stands for the Stefan-Boltzman constant and k^* is the mean absorption coefficient. The thermophysical characteristics of the nanofluid with nanoparticle concentration χ are defined as [6, 7].

$$\left.\begin{aligned}&\mu_{nf}=\frac{\mu_f}{(1-\chi)^{2.5}},\rho_{nf}=(1-\chi)\rho_f+\chi\rho_s,\\&(\rho\beta)_{nf}=(1-\chi)(\rho\beta)_f+\chi(\rho\beta)_s,\alpha_{nf}=\frac{\kappa_{nf}}{(\rho C_p)_{nf}}\\&(\rho C_p)_{nf}=(1-\chi)(\rho C_p)_f+\chi(\rho C_p)_s\end{aligned}\right\} \tag{4}$$

where ρ_{nf} denotes the density of the nanofluid with ρ_f and ρ_s are the densities of primary fluid and nanoparticles respectively; μ_{nf} represents the dynamic viscosity of the nanofluid, α_{nf} signifies the thermal diffusivity of the nanofluid; $(\rho C_p)_f$ and $(\rho C_p)_s$ are the heat capacity of the primary fluid and nanoparticles respectively; β_f and β_s conveys the coefficients of thermal expansion of the primary fluid and nanoparticles respectively.

Maxwell [26] first developed a physical model to establish the effectiveness of thermal conductivity κ_{nf} of nanofluid and is specified by

$$\frac{\kappa_{nf}}{\kappa_f}=\frac{(\kappa_s+2\kappa_f)-2\chi(\kappa_f-\kappa_s)}{(\kappa_s+2\kappa_f)+2\chi(\kappa_f-\kappa_s)}. \tag{5}$$

Here, κ_f and κ_s are the thermal conductivity of the primary liquid and nanoparticle, respectively.

The physics of the problem suggests the following boundary conditions

$$u=0\,,v=\pm v_w(x)\,,T=T_w\,,\text{ at } y=0 \tag{6}$$

$$u\to u_\infty,\quad T\to T_\infty\,,\text{ as } y\to\infty\,. \tag{7}$$

Near the boundary region the velocity component, $v=\pm v_w(x)$ with $v_w(x)=v_0/\sqrt{x}$ is the velocity of suction ($v_0>0$) or injection ($v_0<0$) of the fluid.

We now introduce the stream functions ψ and the similarity transformations as follows:

$$u = \frac{\partial \psi}{\partial y}, \quad v = -\frac{\partial \psi}{\partial x} \tag{8}$$

$$\theta = \frac{T - T_\infty}{T_w - T_\infty}, \quad \eta = y\sqrt{\frac{u_\infty}{\nu_f x}}, \quad \psi = \sqrt{u_\infty \nu_f x}\, f(\eta). \tag{9}$$

Using the relations Eqs. (8) and (9) the governing Eqs. (1)-(3) reduce to

$$f''' + (1-\chi)^{2.5}\left[\begin{array}{l} 0.5ff''\left(1-\chi+\chi\dfrac{\rho_s}{\rho_f}\right) \\ +\left(1-\chi+\chi\dfrac{(\rho\beta)_s}{(\rho\beta)_f}\right)\lambda\theta\cos\Omega \\ -K_1\left(1-\chi+\chi\dfrac{\rho_s}{\rho_f}\right)(f'-1) \\ -K_2\left(1-\chi+\chi\dfrac{\rho_s}{\rho_f}\right)(f'^2-1) \end{array}\right] = 0 \tag{10}$$

$$\begin{aligned} &\frac{\kappa_{nf}}{\kappa_f}\theta'' + \frac{4}{3}N\left\{(c_T+\theta)^3\theta'\right\}' \\ &+0.5P_r f\theta'\left(1-\chi+\chi\frac{(\rho C_p)_s}{(\rho C_p)_f}\right) = 0 \end{aligned} \tag{11}$$

and the boundary conditions turn into

$$f' = 0, \quad f = f_w, \quad \theta = 1 \quad \text{at} \quad \eta = 0 \tag{12}$$

$$f' = 1, \quad \theta = 0 \quad \text{at} \quad \eta \to \infty. \tag{13}$$

Here $\lambda = gx(\rho\beta)_f (T_w - T_\infty)/u_\infty^2 \rho_f$ conveys the buoyancy parameter. $K_1 = \nu_f / k_0 u_\infty$ symbolizes the parameter of the porous medium and $K_2 = k_0' / \sqrt{k_0}$ describes the inertial parameter. $N = 4\sigma(T_w - T_\infty)^3 / k^*(\rho C_p)_f$ denotes the conduction radiation parameter and $c_T = T_\infty / (T_w - T_\infty)$ is the temperature ratio and is very small by its definition. $P_r = \mu_f (\rho C_p)_f / \rho_f \kappa_f$ conveys the Prandtl number.

The reduced skin friction coefficient C_{fr} is formulated as

$$C_{fr} = \mathrm{Re}_x^{\frac{1}{2}} C_f = \frac{1}{(1-\chi)^{2.5}} f''(0) \tag{14}$$

where $\mathrm{Re}_x = u_\infty x / \nu_f$ conveys the local Reynolds number.

Also, the reduced Nusselt number Nu_r is formulated as

$$Nu_r = Nu(\mathrm{Re}_x)^{-\frac{1}{2}} = -\frac{\kappa_{nf}}{\kappa_f}\theta'(0)\left[1 + \frac{4}{3}N\left(c_T + \theta(0)\right)^3\right]. \tag{15}$$

3. Numerical procedure

The leading system of non-linear ODEs Eqs. (8) and (9) and the associated boundary conditions Eqs. (10) and (11) are numerically tackled by the use of 4[th] order Runge Kutta Fehlberg process with a shooting practice with several step lengths to acquire the numerical upshot independent of Δη. The procedure is continued until we obtain the outcome up to the preferred degree of exactness, namely 10^{-8}. The computations are completed through a program which employs symbolic software Maple 17. The comparison graphs show that temperature (Fig. 2) distributions in the nonexistence of Ag-nanoparticles are in estimable harmony with the available exact solutions of Mukhopadhyay et al. [24].

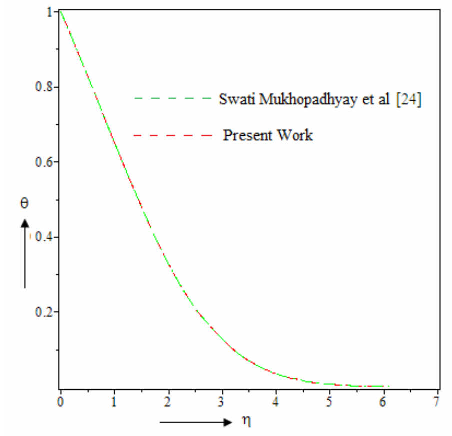

Fig. 2. Comparison of temperature profile.

4. Results and discussion

To visualize the physical insight of this study, the numerical computations have been carried through for range of values of pertinent parameters. To keep on the simulation process the basic values of the parameters are carefully measured as $\chi = 0.15$, $\lambda = 0.2$, $K_1 = 0.1$, $K_2 = 0.1$, $N = 0.2$, $c_T = 0.2$, $P_r = 0.7$, $f_w = 0.5$ unless otherwise specified.

Table 2 represents the impacts of different parameters on the C_{fr} and Nu_r for both the regular fluid and Ag-water nanofluid: Nu_r increases 7.7 % for the regular fluid and 5.8 % for the Ag-nanofluid with increasing the values of K_1 from 0.0 to 1.5 whereas, C_{fr} enhances 85.7 % for regular water and 91.6 % for Ag-water for same ranges of K_1. One may note that as K_2 enlarges from 0.0 to 1.5, Nu_r for regular fluid and Ag-water obtain the growth of 10.2 % and 7.6 %, respectively. With increasing the values of inclination angle Ω from 0^0 to 60^0, C_{fr} decreases 11.25 % for primary fluid and 6.4 % for Ag-nanofluid but impact is not significant for the rate of heat transport. An effective result is observed for N from 0.0 to 1.0. Nu_r increases 80 % for Ag-nanofluid whereas 37.2 % for regular fluid. Also, the rate of shear stress enlarges a lot for Ag-water with N. Nu_r increases with the increment of suction parameter from whereas the result is reverse in case of injection. Nu_r gets a growth of 51.3 % and C_{fr} receives 81.5 % enhancement for Ag-nanofluid model with f_w.

The impact of suction/injection parameter f_w on the velocity distribution is presented in Fig. 3. With the mounting values of suction parameter, the horizontal velocity is found to enhance whereas an opposite effect occurs for injection parameter. The

Table 1. Thermophysical properties of fluid and nanoparticles.

Physical properties	Regular fluid (Water)	Ag
$\rho(kg/m^3)$	997.1	10500
$C_p(J/kg\ \ K)$	4179	235
$\kappa(W/m\ \ K)$	0.613	429
$\beta\times10^{-5}(K^{-1})$	21	1.89

Table 2. Effects of physical parameters on Nu_r and C_{fr}.

K_1	K_2	Ω	N	f_w	Nu_r		C_{fr}	
					Regular fluid	Ag-water	Regular fluid	Ag-water
0.0	0.1	45	0.5	0.5	0.545782	0.908034	0.828883	1.525428
0.5	-----	-----	-----	-----	0.566697	0.934612	1.123845	2.108771
1.5	-----	-----	-----	-----	0.587688	0.960389	1.539494	2.923000
0.1	0.0	45	0.5	0.5	0.542351	0.903614	0.801621	1.471794
----	0.5	-----	-----	-----	0.573004	0.942559	1.193802	2.246907
----	1.5	-----	-----	-----	0.597813	0.972676	1.704048	3.246019
0.1	0.1	0^0	0.5	0.5	0.557867	0.921038	0.959693	1.724719
---	-----	30^0	-----	-----	0.554863	0.918300	0.931163	1.695474
----	-----	60^0	-----	-----	0.550266	0.910624	0.851680	1.614680
0.1	0.1	45	0.0	0.5	0.460918	0.617210	0.874950	1.648335
----	-----	-----	0.5	-----	0.551202	0.915004	0.896941	1.660560
----	-----	-----	1.0	-----	0.632181	1.113379	0.911906	1.669844
0.1	0.1	45	0.5	-0.5	0.329241	0.604794	0.601349	0.915041
-----	-----	-----	-----	-0.1	0.411998	0.725362	0.710650	1.181104
----	-----	-----	-----	0.1	0.456525	0.787537	0.769947	1.331339
	-----	-----	-----	0.5	0.551202	0.915004	0.896941	1.660560

thermal boundary layer width is quicker for Ag-water compared to primary fluid. The impact of the solar radiation on $f'(\eta)$ of an electrically conducting fluid flow over a permeable plate is presented in Fig. 4. For η > 0, the velocity distribution throughout the boundary layer enlarges with the escalating values of N. Fig. 5 illustrates that the increment or decrement of velocity distribution is proportional with χ. The impacts of porosity parameter and inertial parameters on velocity profile are illustrated through the Figs. 6 and 7, respectively. It is found from figures that the momentum boundary layer width enhances a lot for Ag-nanofluid compared to primary fluid with increasing values of porosity parameter K_1 and inertial parameter K_2. The influence of plate inclination angle Ω on $f'(\eta)$ is demonstrated in Fig. 8 and it is vividly clear that the velocity profile lessen as the inclination angle Ω enhances.

Fig. 9 demonstrates that $\theta(\eta)$ reduces with the growing values of suction parameter while, the contrary effect is noticed for injection parameter. Thus the rate of heat transport declines with the rise of suction parameter f_w whereas, for injection the opposite effect occurs. It can be easily verified from Fig. 10 that with the same improvement of N the temperature profile grows significantly for Ag-nanofluid. This is vividly notified from Fig. 11 that the dimensionless temperature profile augments with the lofted value of χ. This occurs

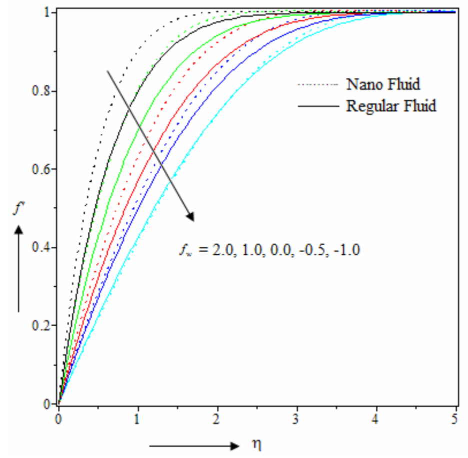

Fig. 3. Velocity profile for suction / injection parameter f_w.

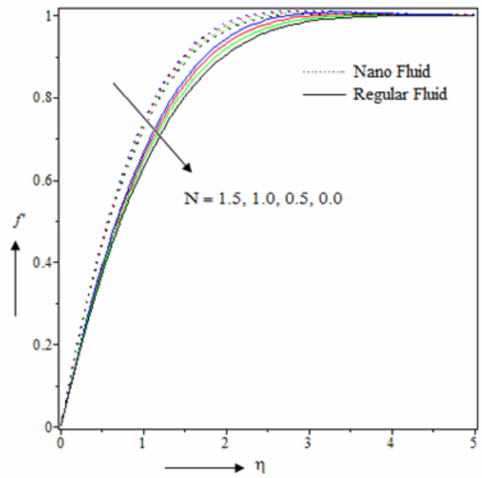

Fig. 4. Velocity profile for solar radiation parameter N.

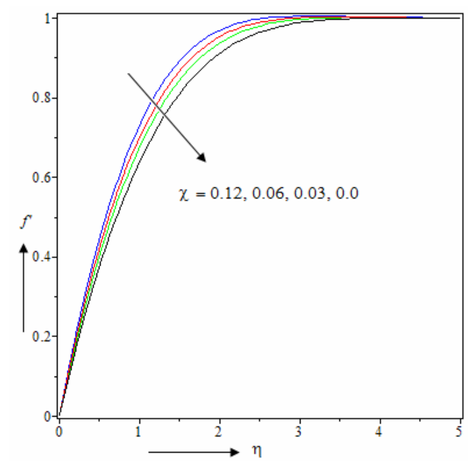

Fig. 5. Velocity profile for nanoparticle volume fraction χ.

owing to the high thermal conductivity of the Ag nanoparticles which enhance of heat absorbing capability of the regular fluid. Figs. 12 and 13 represent the Darcy-Forchheimer effect

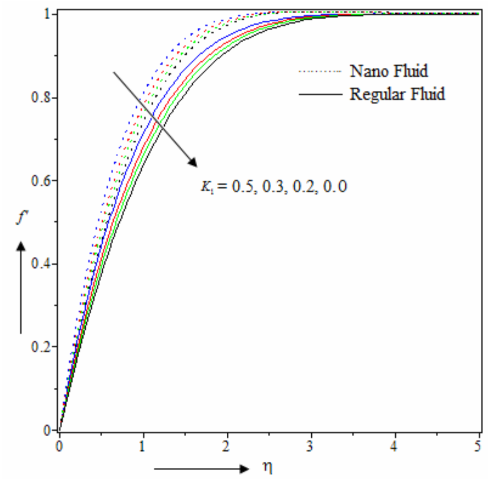

Fig. 6. Velocity profile for porosity parameter K_1 .

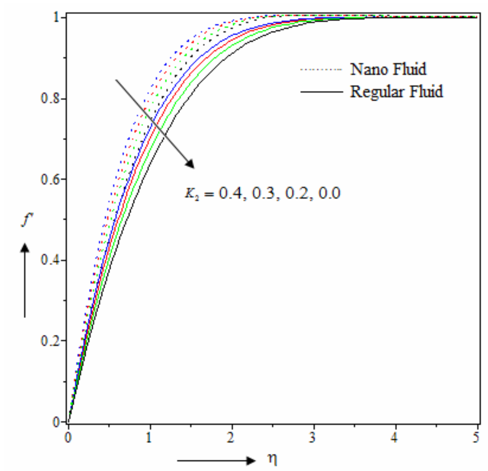

Fig. 7. Velocity profile for inertial parameter K_2 .

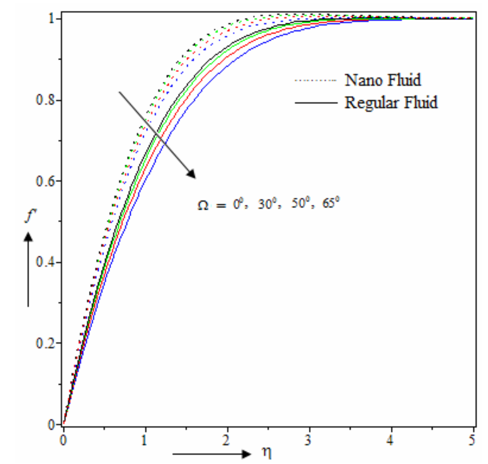

Fig. 8. Velocity profile for inclination angle Ω .

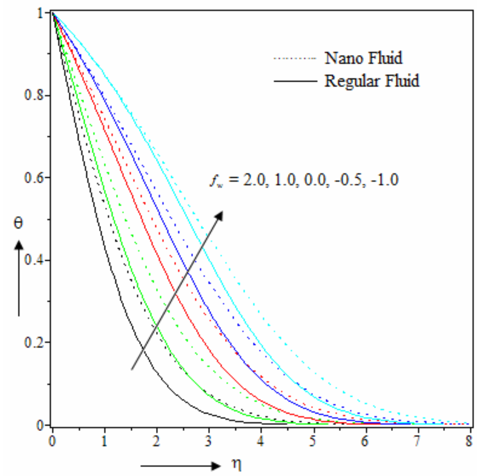

Fig. 9. Temperature profile for suction / injection parameter f_w .

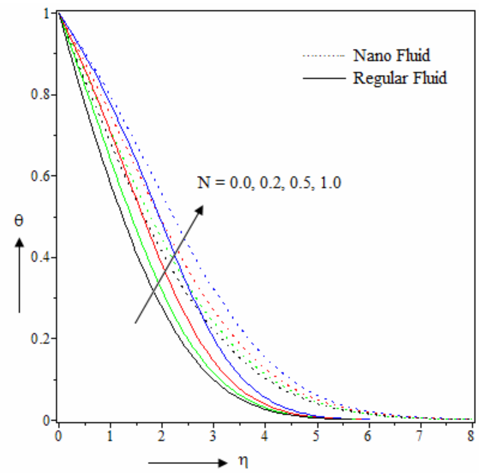

Fig. 10. Temperature profile for solar radiation parameter N .

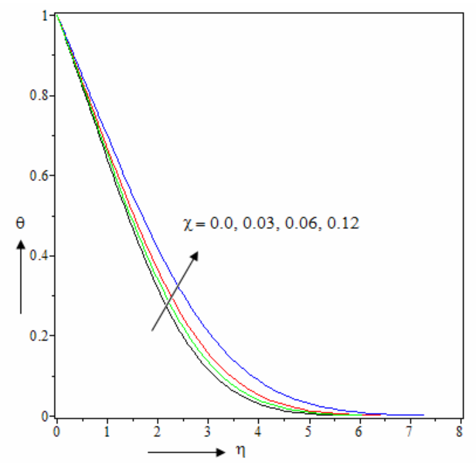

Fig. 11. Temperature profile for nanoparticle volume fraction χ .

on the temperature profiles coexistence of solar radiation. It should be noteworthy that with the escalating values of the porosity parameter K_1 and the inertial parameter K_2, the temperature decays.

5. Conclusions

A mathematical model is proposed to analyze the impact of solar radiation on natural convection flow of Ag-water nan-

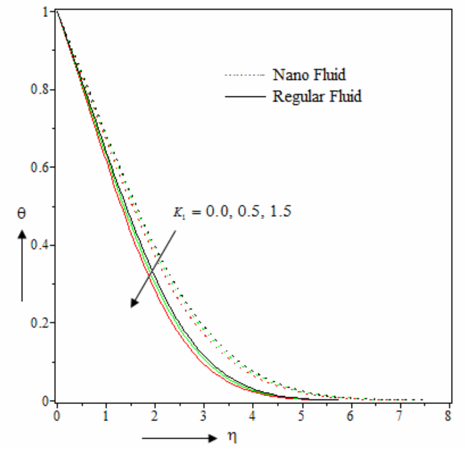

Fig. 12. Temperature profile for porosity parameter K_1.

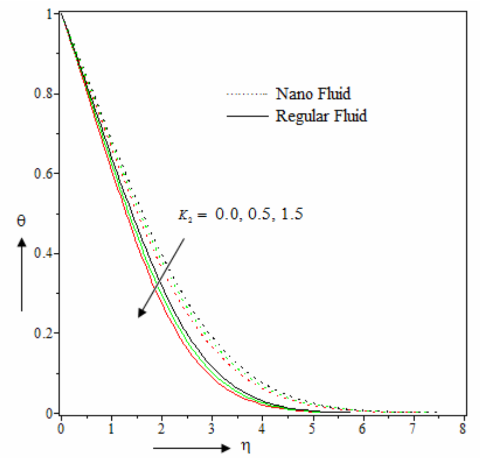

Fig. 13. Temperature profile for inertial parameter K_2.

ofluid over an inclined permeable plate embedded in a Darcy-Forchheimer porous medium. The leading equations are numerically solved and the graphical fallouts are obtained to demonstrate the details of flow behavior. At the finale we arrive to the following deduction:

- The width of momentum boundary layer widen rapidly with the mounting values of solar radiation parameter coexistence of Ag-nanofluid compared to water whereas, reverse effect occurs for inclination angle of the plate.
- Temperature boundary layer width decays with permeability parameter and inertial parameter but reverse effect is notified for solar radiation parameter.
- In presence of Ag-nanoparticles the growth of Nusselt number lessens compared to regular water whereas Skin friction enlarges significantly high with Ag-nanofluid.

Acknowledgement

The authors want to articulate their pleasant gratitude to reviewers for their precious propositions and remarks to improve the article.

References

[1] A. J. Hunt, Small particle heat exchangers, Lawrence Berkeley Laboratory report no. LBL 7841, *Journal of Renewable Sustainable Energy* (1978).

[2] S. Choi, Enhancing thermal conductivity of fluids with nanoparticles. 66, D. A. Siginer, H. P. Wang (Eds.), Developments and Applications of Non-Newtonian Flows, *ASME MD*, FED, 231(1995) 99-105.

[3] A. V. Kuznetsov and D. A. Nield, Natural convective boundary-layer flow of a nanofluid past a vertical plate, *International Journal of Thermal Science*, 49 (2010) 243-347.

[4] J. Buongiorno and W. Hu, Nanofluid coolants for advanced nuclear power plants, Paper no. 5705, *Proceedings of ICAPP,* Seoul, 5 (2005) 15-19.

[5] M. A. Hossain and H. S. Takhar, Radiation effect on mixed convection along a vertical plate with uniform surface temperature, *International Journal of Heat Mass Transfer*, 31 (1996) 243-248.

[6] R. Kandasamy, I. Muhaimin, A. B. Khamis and R. Roslan, Unsteady Heimenz flow of Cu-nanofluid over a porous wedge in the presence of thermal stratification due to solar energy radiation: Lie group transformation, *International Journal of Thermal Science*, 65 (2013)196-205.

[7] K. Das, P. R. Duari and P. K. Kundu, Solar radiation effects on Cu-water nanofluid flow over a stretching sheet with surface slip and temperature jump, *Arabian Journal for Science and Engineering,* 39 (2014) 9015- 9023.

[8] R. K. Tiwari and M. K. Das, Heat transfer augmentation in a two sided lid-driven differentially heated square cavity utilizing nanofluids, *International Journal of Heat and Mass Transfer*, 50 (2007) 2002-2018.

[9] X. Q. Wang and A. S. Mujumder, Heat transfer characteristics of nanofluids: A review, *International Journal of Thermal Science*, 46 (2007) 1-19.

[10] E. Abu-Nada, Application of nanofluids for heat transfer enhancement of separated flows encountered in a backward facing step, *International Journal of Heat Fluid Flow*, 29 (2008) 242-249.

[11] H. F. Oztop and E. Abu-Nada, Numerical study of natural convection in partially heated rectangular enclosures filled with nanofluids, *International Journal of Heat Fluid Flow*, 29 (2008) 1326-1336.

[12] S. Karak and A. Pramuanjaroenkij, Review of convective heat transfer enhancement with nanofluids, *International Journal of Heat and Mass Transfer*, 52 (2009) 3187-3196.

[13] K. Das, Slip flow and convective heat transfer of nanofluids over a permeable stretching surface, *Computers and Fluids*, 64 (2012) 34-42.

[14] M. Moslehi and M. Saghafian, MHD mixed convection slip flow in a vertical parallel plate microchannel heated at asymmetric and uniform heat flux, *Journal of Mechanical Science and Technology*, 29 (2015) 5317-5324.

[15] M. Azimi and R. Riazi, MHD copper-water nanofluid flow and heat transfer through convergent-divergent channel,

Journal of Mechanical Science and Technology, 30 (2016) 4679-4686.
[16] P. Cheng and W. Minkowycz, Free convection about a vertical flat plate embedded in a porous medium with application to heat transfer from a dike, *Journal of Geophysical Research*, 82 (1977) 2040-2044.
[17] F. C. Lai and F. A. Kulacki, Non- Darcy mixed convection along a vertical wall in a saturated porous medium, *International Journal of Heat and Mass Transfer*, 113 (1991) 252-255.
[18] K. Vafai and C. L. Tien, Boundary and inertia effect on convection mass transfer in porous media, *International Journal of Heat and Mass Transfer*, 25 (1982) 1183-1190.
[19] J. T. Hong, Y. Yamada and C. L. Tien, Effects of non-Darcian and non-uniform porosity on vertical plate natural convection in porous media, *ASME Journal of Heat Transfer*, 109 (1987) 356-362.
[20] M. Kaviany, Boundary layer treatment of forced convection heat transfer from a semi infinite flat plate embedded in porous media, *ASME Journal of Heat Transfer*, 109 (1987) 345-349.
[21] K. S. Chen and J. R. Ho, Effects of flow inertia on vertical natural convection in saturated porous media, *International Journal of Heat and Mass Transfer*, 29 (1988) 753-759.
[22] Y. J. Rami, A. Fawzi and F. A. Rub, Darcy-Forchhimer mixed convection heat and mass transfer in fluid saturated porous media, *International Journal of Numerical Methods for Heat & Fluid Flow*, 11 (2001) 600-618.
[23] A. Ishak, Similarity solutions for flow and heat transfer over a permeable surface with convective boundary conditions, *Applied Mathematics and Computation*, 217 (2010) 837-842.
[24] S. Mukhopadhyay, P. R. De, K. Bhattacharyya and G. C. Layek, Forced convective flow and heat transfer over a porous plate in a Darcy-Forchhimer medium in presence of radiation, *Meccanica*, 47 (2012)153-161.
[25] K. A. Fathalah and M. M. Elsayed, Natural convection due to solar radiation over a non absorbing plate with and without heat losses, *International Journal of Heat and Fluid Flow*, 2 (1980) 41-45.
[26] J. C. A. Maxwell, *A Treatise on electricity and magnetism, 2 unabridged*, Third Ed., Clarendon Press, Oxford, UK (1891).

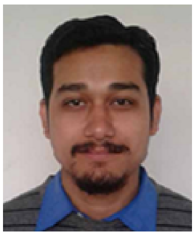

Tanmoy Chakraborty has completed his M.Sc. degree in Applied Mathematics from the University of Calcutta in 2012. Now he is going to complete Ph.D. degree from Jadavpur University. So far he had 3 research papers published in International journals in the fields of fluid mechanics (MHD and Nanofluids). He is now working as an Assistant Professor in Techno India College of Technology, West Bengal, India.